

Fade Depth Prediction Using Human Presence for Real Life WSN Deployment

Goran HORVAT, Snježana RIMAC-DRLJE, Drago ŽAGAR

Dept. of Communications, J.J. Strossmayer University of Osijek, Kneza Trpimira 2b, 31000 Osijek, Croatia

goran.horvat@etfos.hr, rimac@etfos.hr, drago.zagar@etfos.hr

Abstract. *Current problem in real life WSN deployment is determining fade depth in indoor propagation scenario for link power budget analysis using fade margin parameter. Due to the fact that human presence impacts the performance of wireless networks, this paper proposes a statistical approach for shadow fading prediction using various real life parameters. Considered parameters within this paper include statistically mapped human presence and the number of people through time compared to the received signal strength. This paper proposes an empirical model fade depth prediction model derived from a comprehensive set of measured data in indoor propagation scenario. It is shown that the measured fade depth has high correlations with the number of people in non-line-of-sight condition, giving a solid foundation for the fade depth prediction model. In line-of-sight conditions this correlations is significantly lower. By using the proposed model in real life deployment scenarios of WSNs, the data loss and power consumption can be reduced by the means of intelligently planning and designing Wireless Sensor Network.*

Keywords

Fade depth prediction, human presence, human density, received strength signal indicator, wireless sensor networks, ZigBee.

1. Introduction

Signal fading presents a recurring problem for reliable wireless communication. It affects system's performance and must be taken into consideration for real life deployment of Wireless Sensor Networks (WSNs). In wireless communications, fading is a deviation of the attenuation that a carrier-modulated telecommunication signal experiences over certain propagation media. Fading varies with time, geographical position and/or radio frequency and is modeled as a random process. Fading can be caused by multipath propagation, so called multipath fading, or caused by shadowing from obstacles present on the radio path, sometimes referred to as shadow fading [1]. In this

paper we discuss shadow fading caused by human presence and its impact on WSN signal propagation.

An accurate estimation of fade depth is of great importance upon designing reliable Wireless Sensor Network. Due to the fact that numerous parameters can contribute to the loss of signal power at the receiver's side (i.e. Radio irregularity, impact of other wireless equipment, the presence of obstacles in the propagation path and others) this paper proposes the use of fading margin for real life WSN deployment. Most of the models for signal fading prediction used in the microwave wireless link budget analysis are mainly empirical in nature and often rely on extensive measured data [2]. Our approach is transformed into Wireless Sensor Network budget analysis proposed by this paper. On the other hand, the existing models include aggregate effects of different fading mechanisms and do not allow for any insight into relative importance of these mechanisms. In this paper the fading mechanisms are explained through a statistical point of view. This is supported by various papers where authors emphasize the impact of radio irregularity from human presence [4], [5].

From an empirical point of view the impact of human presence could be shown in correlation with the drop in received signal strength of the receiving node. This is demonstrated throughout extensive set of measurements. The magnitude of the signal drop is examined versus the number of people in a designated area. Further on, by examining the statistical nature of the data, this paper proposes the human presence factor, describing the number of people occupying an area within the signal propagation path. By comparing human presence against the magnitude of the received signal drop it is possible to determine the fading margin for the given communication link. Further on, by implementing WSN budget link analysis it is possible to reduce transmit power of the WSN sensor nodes thus reducing the overall consumption of the sensor nodes. Consequently, possible side effects of electromagnetic field on human health are reduced accordingly.

In the following Section, the related work and the fading margin RF budget link analysis are described. In Section 3 testbed for statistical analysis and RF analysis is presented, whereas Section 4 proposes an empirical model. Section 5 gives the conclusion.

2. Fade Depth Prediction in WSN

Shadow fading is a phenomenon that occurs when a mobile receiver moves behind an obstruction and experiences a significant reduction in signal power (Fig. 1). On the other hand, in stationary WSN shadow fading occurs when an obstacle gets positioned between the wireless device and the signal transmitter. This interference causes significant reduction in signal strength because the wave is shadowed or blocked by the obstacle [6], [7].

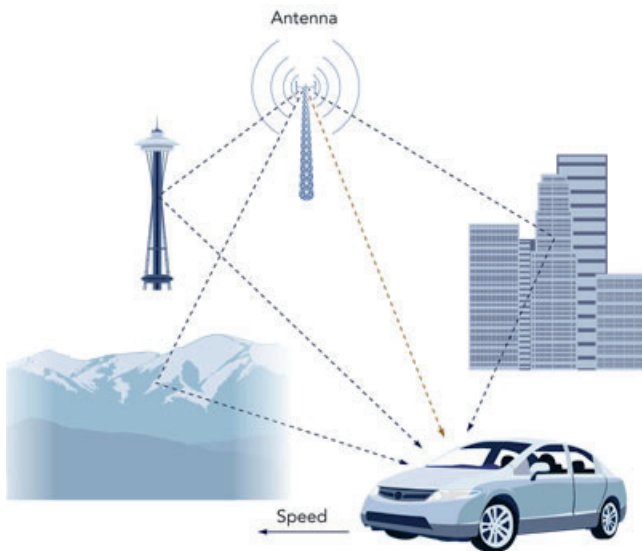


Fig. 1. Signals experience fading during transmission. Obstacles such as buildings and mountains reflect or absorb the signals.

When analyzing the impact of shadow fading in Wireless Sensor Networks, one of the most important scenarios for WSN deployment is the indoor scenario. Here the nodes are distributed inside of a building or a building complex where various factors influence the RF propagation.

Since WLAN (Wireless Local Area Networks) networks and WSN networks operate within the same ISM band of 2.4 GHz, the same principles for WLAN apply for the WSN, only difference being the different bandwidth of RF channels [9], [10]. According to [8], the RF propagation path of a WLAN network crosses various obstacles (furniture, people etc.) resulting in net effect that is an attenuation caused by static obstacles and a more varying signal due to moving obstacles such as moving people. As a consequence, there are rapid and frequent transitions between (LOS) line-of-sight and (NLOS) non-line-of-sight conditions, causing a variation in the statistics of fast fading, which is closely associated with the shadowing process. The characteristic of shadowing caused due to moving people resembles fast fading in propagation environments. From the modeling point of view, it is more convenient to treat people shadowing and narrowband fast fading as a single entity – a closely coupled process, in which the parameters of fading and shadowing are time-varying.

2.1 Related Work

Related work on the subject of fade depth prediction varies extensively throughout the literature. The most common use of fade depth prediction is for the purpose of RF link budget analysis [2]. The most common use of RF budget analysis encompasses the planning of microwave RF links.

Due to the interesting approach of using fade margin for network planning, the same principle could be applied to the Wireless Sensor Network area of research. According to [3], the authors present an approach of modeling a WSN according to RF budget link analysis and fade margin parameter for 915 MHz band. The proposed work encompasses the overall impact of multipath and shadow fading in order to calculate fading depth and accordingly the minimum transmit power of a node. On the other hand, no correlation of human presence with the drop of received strength is shown.

Further on, the authors in [4] and [5] express the impact of human presence on the RF propagation of a Wireless Sensor Network. The paper evaluates the performance in indoor line-of-sight (LOS) and non-line-of-sight (NLOS) conditions through a detailed analysis of Received Signal Strength Indicator (RSSI) measurements. The results indicated by the authors suggest that during the day period, the human activity has a significant impact on the performance of indoor wireless networks, whereas, during the night period, radio links are stable with little fluctuations, correlating with human presence. On the other hand, the authors do not present any form of exploiting the acquired findings for implementation in real life deployment scenarios by proposing a real life deployment model. Further on, the authors do not investigate the impact of human density on the propagation, presenting a drawback. In our paper a deployment model based on link budget analysis was proposed so that by using statistical parameters it is possible to determine minimum power levels for WSN nodes in certain conditions.

Next on, the work presented in [8] describes in detail indoor channel models accounted for the impact of human presence. The model described by the authors represents channel statistics in terms of parametric distributions, which can be approximated by a combination of Rice, Rayleigh and Log Normal components. According to [8] a narrowband fading in indoor environment can be represented as a combination of two distinct parts: a coherent path (the result of the direct line-of-sight path) and a diffuse part (arising from large number of non-line-of-sight components in different phases). The authors clearly state the effect the human presence has on the propagation. However, the paper does not propose any form of real life deployment model based on the transmit power. Also, the proposed testbed is based on WLAN systems that differ from WSN systems in deployment, position and mobility.

Finally, the authors in [11] approach the multipath fading problem from a deterministic point of a view. From

various experimental and simulation results, the authors emphasize that fading is a spatial phenomenon. Wireless links provide a constant packet delivery performance when there is no interference and the conditions are static. Time variations in signal strength only occur if the wireless terminals are moving or in the case of external disturbances. However, according to the measurements conducted in our paper, static conditions such as static human presence can interfere with the packet delivery performance, so this aspect needs to be examined in detail.

When analyzing WSN modules, the modules used for measurements in this paper were described in detail in the literature. In [13] the authors present a basic testbed for measurements where the emphasis is given on RSSI parameters and data reception rate. The authors in [13] give the basic analysis on propagation in various LOS and NLOS conditions. Also, the approach of using a fade depth margin is stated as one of the options for real life WSN deployment and the direct influence of human presence on the WSN nodes is shown.

The novelty of our approach is the introduction of the human density factor with the empirical approach in order to calculate minimum power level for a WSN node. Compared to the related work, our approach uses statistical parameters of human density to define fading depth parameter and intelligently plan the WSN. After defining the fade depth for a RF link, it is possible to design a WSN network regarding transmit power, directly impacting the power consumption and RF spectrum contamination.

3. The Measurement Testbed

To analyze the impact between human activity and RF propagation of WSN nodes, the testbed was proposed in real life indoor scenario. The testbed was composed of several components that in conjunction results in a comprehensive system capable of synchronously processing vast amounts of data. The complete system could be divided into three major components: Wireless Sensor Network, Propagation analysis system and People counting system. From an analytical point of a view, the Wireless Sensor Network is the object being analyzed whereas the propagation analysis and the people detection systems are the means of deriving statistically valuable data on the topic of the WSN deployment.

3.1 Wireless Sensor Network Setup

The first and foremost component of the analytical testbed is the Wireless Sensor Network, being the object of the research. The WSN testbed in this paper consisted of five wireless sensor nodes linked to the network coordinator. The network topology used in the testbed is based on a *ZigBee* protocol implemented by the used WSN nodes. The used nodes are *Digi's XBee* nodes consisting of IEEE802.15.4 PHY and MAC layers and higher *ZigBee*

layers in the stack [17]. *ZigBee* network topology consists of three types of nodes: coordinator, router and end node having the following functionality: establishing a network, routing messages to adjacent nodes and transferring acquired data, respectively. In the proposed testbed only two types of nodes were used: coordinator and end node. By excluding the router node from the testbed, direct links from end nodes to the coordinator are forced, thus giving a static network configuration and static propagation paths.

The first four nodes were in direct link with the testbed, whereas the fifth node was arbitrarily placed within the building. Floor plan of the testbed is shown in Fig. 2.

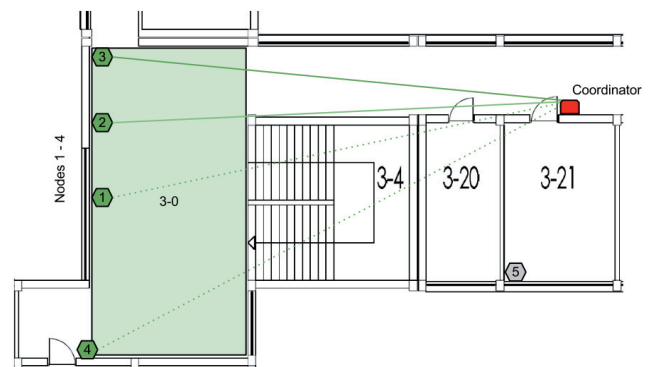


Fig. 2. Floor plan of the WSN testbed.

As seen from Fig. 2, two nodes are located in the line-of-sight (LOS) situation, whereas the remaining nodes exhibit the non-line-of-sight (NLOS) condition. The area noted as 3-0 was chosen for the versatile distribution of people density throughout the day. The nodes are located at a height of 1 m from the floor, whereas the coordinator is set at 3 m, respectively. To facilitate real life conditions, the WSN hardware configurations were chosen according to RF transmit power, Antenna gain and the type of WSN node. Tab. 1 depicts the hardware configuration.

Node ID	RF power [dBm]	Antenna Gain [dBi]	XBee Node Type	Condition
1	3	4	Series 2	NLOS
2	10	2	S2B PRO	LOS
3	10	2	S2B PRO	LOS
4	17	1.8	XBee PRO	NLOS
5	3	1.8	Series 2	NLOS
coordinator	10	2.1	S2 PRO	-

Tab. 1. WSN nodes specifications [12], [17] and [18].

As seen from Tab. 1 the hardware configuration enables the testing under real life conditions as it represents various combinations of transmit power, antenna gains and propagation conditions.

3.2 Propagation Analysis System

After setting the testbed for the WSN nodes, the backbone infrastructure for data acquisition was estab-

lished. Since the proposed network configuration consists of five WSN end nodes and one coordinator, the data acquisition system was developed as such a coordinator periodically polled every end node for status. The polled status included the received signal strength expressed in dBm for both the coordinator and the designated end node, representing the key information for this testbed scenario.

To implement the required functionality and to avoid the use of a personal computer functioning as a data acquisition system, an embedded system named *ConnectPort X4* was used instead. The used embedded system is an ARM based device supporting *Python* scripting and functioning as a Gateway between the *ZigBee* PAN and the *Internet*. To avoid the need for a database, an online *Cloud* storage was used in the form of *Google Apps Cloud* computing service (Fig. 3).

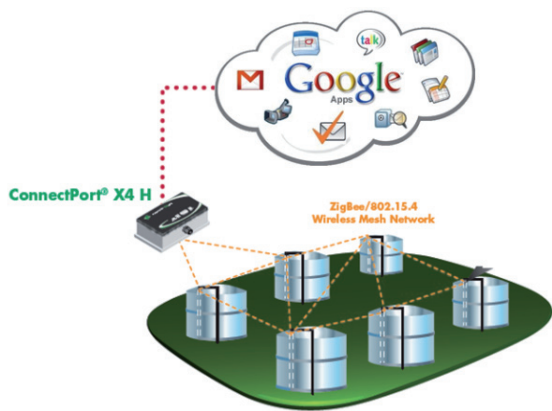


Fig. 3. Interconnection between WSN and Cloud data storage.

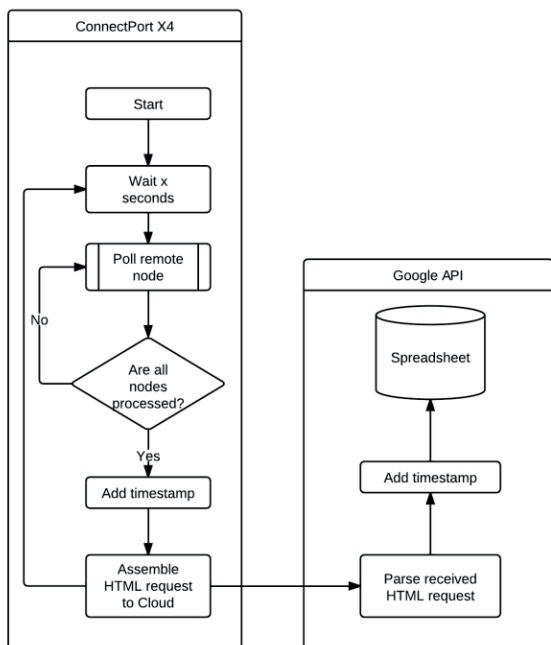


Fig. 4. Flow diagram for the Propagation analysis system.

By using the proposed architecture, the data integrity is secure within the *Cloud* service, and the need to develop custom Ad Hoc PC applications is avoided. Fig. 4 shows

the flow diagram for polling the remote WSN nodes and delivering the data to the *Cloud*. The algorithm is implemented within *ConnectPort X4* Python scripting language and the data is periodically polled from the side of the *ConnectPort X4*.

As seen from Fig. 4, the power levels values for all WSN nodes are acquired after which the data is sent to the Google Cloud (Spreadsheet) service. The method of sending the data consists of assembling a HTTP request where the data is passed as parameters in the URL (e.g. "https://docs.google.com/macros/exec?service=AKfycbyJSvLP2rqLE9tk85u6KzXTorHh1dY4rA9zdQdmzQ&RSSI_N1=%s&RSSI_C1=%s&RSSI_N2=%s&RSSI_C2=%s&RSSI_N3=%s&RSSI_C3=%s&RSSI_N4=%s&RSSI_C4=%s&RSSI_N5=%s&RSSI_C5=%s&Time=%s"). The data is stored in the Cloud service and is available in real time to the end user.

3.3 People Counting System

In order to complete the proposed measurement testbed, the need to count the number of people habiting the test area is expressed. To count the number of people habiting the test area 3-0 from Fig. 2, several solutions have been revised, from the simplest solution of IR beam crossing to the most sophisticated methods including thermal vision identification. The method of choice in this paper is a video detection method. The used method is adapted from [19], [20] and similar work based on blob detection. The video detection of human presence in the designated area is shown in Fig. 5 a) and b).



Fig. 5. Detecting number of persons in the monitored area by the means of video processing.

From the processed results of the video detection algorithm compared to the manually counted persons for a random number of intervals, it was concluded that the accuracy of the detection algorithm varies from 100% (for lower number of people) to approximately 80% (for a larger number of people). Accordingly, for critical time peri-

ods of higher activities the number of persons was manually corrected to reduce the statistical uncertainty.

By implementing people counting system the proposed testbed is complete. The sets of measurements was conducted, a vast number of data was collected over an extended period of time, statistically processed and analyzed in the means of defying a correlation between the RF attenuation and the number of persons in the controlled area.

4. Representing Fading Margin Related to Human Presence

4.1 RF Propagation

In order to represent the fading margin, the received signal strength at the receiver side must be represented. The received signal strength is presented as [15]:

$$P_R [\text{dBm}] = P_T [\text{dBm}] + G_T [\text{dB}] + G_R [\text{dB}] - L_{Pr} [\text{dB}] \quad (1)$$

where P_R and P_T are received and transmitted power correspondingly, G_R and G_T are receive and transmit antenna gains correspondingly and L_{Pr} is the propagation channel loss usually factored into three main components:

$$L_{Pr} [\text{dB}] = L_{pl} [\text{dB}] + L_S [\text{dB}] + L_L [\text{dB}] \quad (2)$$

where L_{pl} is the average path loss (e.g. multiwall model), L_L is the long-term fading (e.g. due to the shadowing of people presence), and L_S is the short-term fading (due to multipath). Hence, the fade margin can be defined as:

$$F [\text{dB}] = L_S [\text{dB}] + L_L [\text{dB}] \quad (3)$$

The transmitter power or the transmitter or receive antenna gains must be increased by F to sustain the reliable link operation as compared to the case of un-faded propagation channel [2]. For the Wireless Sensor Networks propagation scenario, additional obstacles are people moving through the area crossing the radio paths. Therefore the human presence influences long-term as well as short term fading.

For indoor propagation scenarios, average path loss models vary in design and accuracy. One of the most commonly used models for average path loss in indoor scenarios is the Multi-Wall-and-Floor model (MWF) [16]:

$$L_{MWF} [\text{dB}] = L_0 + 10n \log(d) + \sum_{i=1}^I \sum_{k=1}^{K_{wi}} L_{wik} + \sum_{j=1}^J \sum_{k=1}^{K_{fj}} L_{fjk} \quad (4)$$

where L_0 is path loss at a distance of 1 m, n is power decay index, d is the distance between transmitter and receiver, L_{wik} is attenuation due to wall type i and k -th traversed wall, L_{fjk} is attenuation due to wall type i and k -th traversed floor, I is the number of wall types, J is the number of floor

types, K_{wi} is the number of traversed walls of category i , and K_{fj} is the number of traversed floors of category j . The parameters of the model have been derived by means of ray tracing simulation and can be extracted from the results found in literature [16].

4.2 Experimental Verification of the MWF Model

Within the previous research work documented in [14], the MWF (Multi-Wall-and-Floor) model is experimentally verified against previously measured data. The following figure shows the relation between measurement and MWF model for five locations which differ in the number of walls between transmitter and receiver. Locations are color coded. In each location five additional settings of transmit power were set (points 1 – 5), in order to eliminate the impact of transmit power on the model.

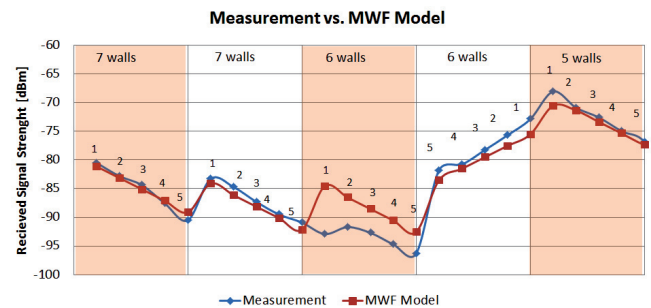


Fig. 6. Measured RSSI values for 5 different locations and 5 different transmit power values

As seen from Fig. 6, the measured data fit the MWF model in majority of situations. In certain scenarios higher amount of deviation is induced that can be attributed to shadowing from obstacles. Further on, it is clearly seen that by varying power levels of the WSN nodes, the MWF model follows the change of power even in scenarios of higher deviation. From the presented it can be concluded that the MWF model is an acceptable model for WSN indoor average path loss.

4.3 Human Presence Density Factor

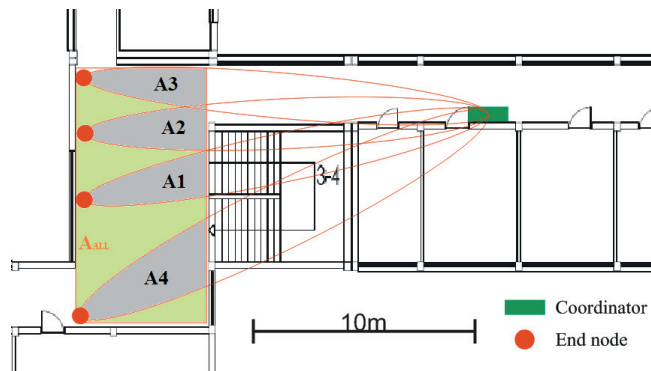


Fig. 7. Effective areas of 1st Fresnel zone propagation paths.

From the related work described in Section 2 A, the impact of human presence on the RF propagation in Wireless Sensor Networks is described throughout various authors. However, to uniquely identify the number of people impacting the propagation, this paper defines effective people density impacting the area of 1st Fresnel zone. The testbed areas are shown in Fig. 7. From Fig. 7 it is clearly seen that the overall area A_{All} is overlapped by the areas encompassed by the 1st Fresnel zone of the propagation. Consequently, human presence density for each node could be defined as:

$$\rho_n = \rho_{All} \frac{A_n}{A_{All}} \quad (5)$$

where ρ_n is the people density for node n , ρ_{All} is the people density thorough entire area A_{All} and A_n is the area of 1st Fresnel zone defined as:

$$A_n = 2\sqrt{\frac{\lambda}{d}} \cdot \left[\int_0^l \sqrt{(d-l)d} dl \right] \quad (6)$$

where λ is the wavelength, d is the distance from node to the coordinator and l is the distance from the node to the end of the observed area derived from the 1st Fresnel zone equation [21]. The testbed areas alongside with the overall observed area are displayed in Tab. 2.

Node ID	Distance from coordinator [m]	1 st Fresnel zone diameter [m]	Area [m ²]
1	18.3	1.52	5.5
2	18.2	1.5	5.5
3	18.6	1.53	5.8
4	20.4	1.6	6.9
Observed area	-	-	60

Tab. 2. Node distance end effective area.

If the overall people density is defined as:

$$\rho_{All} = \frac{n_{people}}{A_{All}}, \quad (7)$$

people density per WSN node is:

$$\rho_n = \frac{A_n \cdot n_{people}}{A_{All}} \quad (8)$$

where n_{people} indicates the number of persons occupying the entire observed area. With the defined human presence density factor it is possible to adequately analyze the influence of human presence on the RF propagation in Wireless Sensor Networks.

5. WSN Propagation Analysis Using People Density Parameter

The proposed testbed for the analysis of the human presence impact on RF propagation was described in Section 3, where the measurement system was explained in detail. Using the measurement testbed the analysis was performed during an extended period of time. In this paper only a segment of the data is displayed. First set of measurements included the static measurements of short-term fading in the scenario without human presence. The statistical parameters are derived from a data set calculated on a moving window. The moving window is sized at 10 samples, representing 50 seconds in real time. This time was chosen as twice the time needed for a person to walk the longest distance in the proposed testbed. Results of received signal strength measurements are shown in Fig. 8.

From Fig. 8 it is visible that in scenario with no human presence the only present fading is low amplitude short-term fading. The cause of this fading can be attributed not to physical characteristics of the communication channel, but to LSB (Least Significant Bit) error due to the 8 bit quantization, of the RSSI value. The toggling of LSB causes the drops and overshoots in the signal strength by 1 dB, whereas other changes can be attributed to the receiver’s physical characteristics.

On the other hand, upon human presence the deviations in the received signal strength are largely expressed. As shown in Fig. 9, standard deviation strongly correlates with the number of people, as seen from the drops in received signal levels. The average RSSI values are displayed alongside with the standard deviation for different number of people (in the observed area) throughout time samples. Difference between time samples is equal to 5 seconds, resulting in overall length of 6.6 hours.

The results shown in Fig. 9 are the results for the nodes with the highest correlation coefficient (nodes 1 and

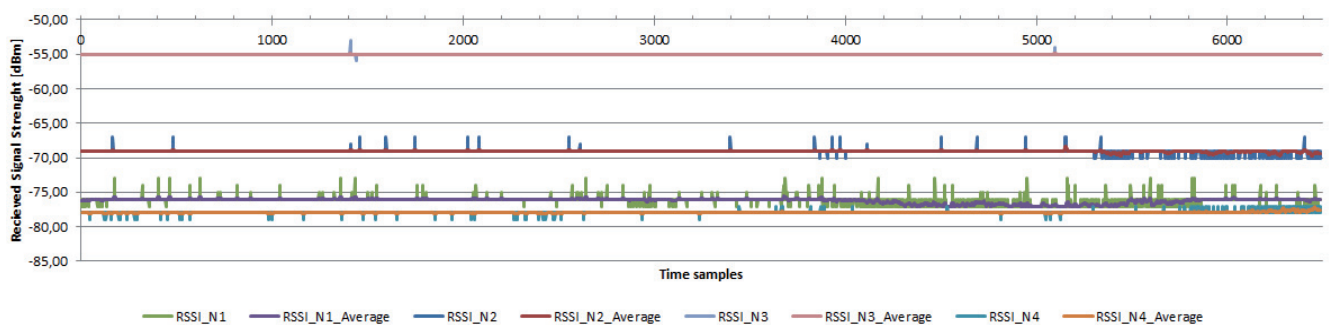


Fig. 8. Received Signal Strength without human presence.

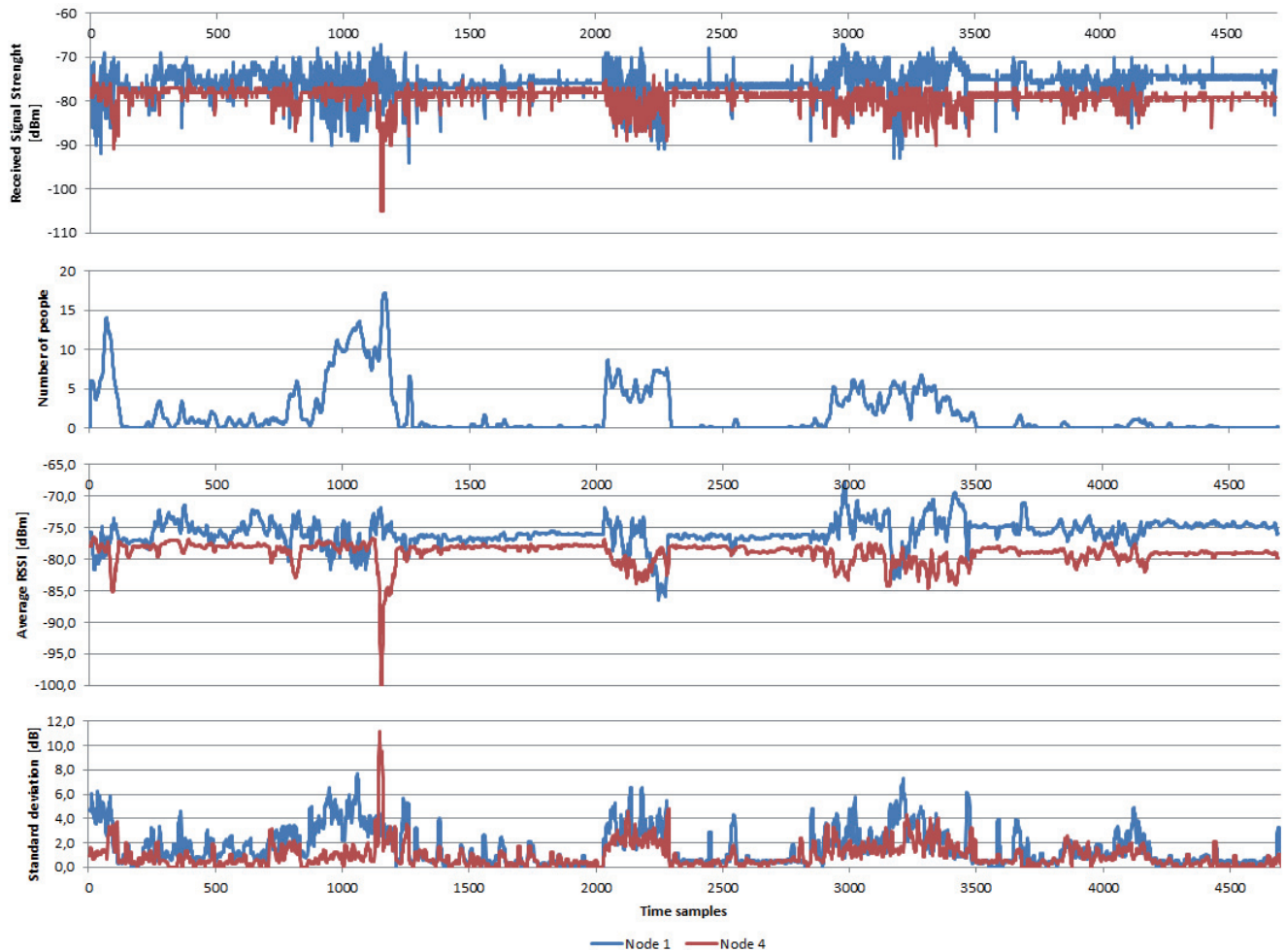


Fig. 9. RSSI Instantaneous values, Number of people, Average values and Standard deviation for nodes 1 and 4 during human presence.

4). Nodes 1 and 4 are exemplifying NLOS conditions. On the other hand, nodes 2 and 3 are exemplifying LOS conditions, where the correlation of the received signal strength with the number of people is not as strong. Comparison of the correlation coefficients for the standard deviation of the received signal strength against the number of people (people density) for nodes 1 through 5 is seen from Fig. 10. The node 5 is not located inside the testbed, on an arbitrary point inside the building, representing a point not in relation with testbed.

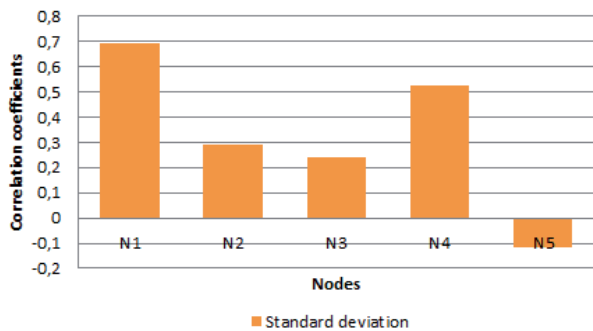


Fig. 10. Correlation coefficients of people density against standard deviation for different nodes.

As seen from Fig. 10 the correlation between received signal’s standard deviation and people density for nodes with NLOS conditions is strong, whereas nodes exhibiting LOS conditions show less correlation. For node 5 that is not in relation with the testbed the correlation coefficient is very low, showing no direct correlation between people density and received signal strength, as expected.

If the comparison is drawn between statistical parameters of the measurements (standard deviation and average value) and the physical signal characteristics (fading), we can identify the short term fading as a standard deviation component and long term fading as the drops in average value of the received signal strength. Consequently, short term fading can be expressed from the standard deviation as:

$$L_s[\text{dB}] = 1.64 \cdot \sigma_s \tag{9}$$

where σ_s is the standard deviation of the data in static setup. Equation (9) is derived from Gaussian distribution with 90% confidence (factor 1.64). From (9) it is possible to calculate short-term fading margins. If the standard deviation is calculated from the data in scenario with no human presence, the resulting data are shown in Tab. 3.

Node ID	Standard deviation [dB]	Short-term fading margin [dB]
1	0.47	0.94
2	0.21	0.44
3	0.03	0.06
4	0.17	0.34
5	0.39	0.78

Tab. 3. Node short-term fading prediction in static conditions.

From Tab. 3 it is visible that short term fading is represented as low amplitude fading in scenario with no human presence. From measured data, short term fading ranges from 0 dB to 1 dB in static conditions. If the same principle is applied to measurements obtained with human presence, the relation between standard deviation and overall people density for node 1 is shown in Fig. 11.

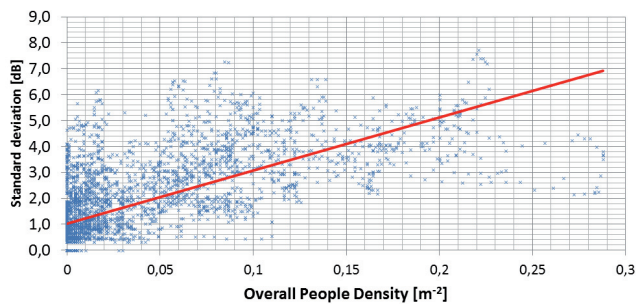


Fig. 11. Standard deviation for node 1 versus overall people density.

Fig. 11 shows a rising trend for standard deviation, as the number of people (people density) increases. This is the result of multipath fading attributed to large number of reflected rays due to the increased people density. This can be predicted using simple linear regression. If compared to other nodes, the same trend is observed (Fig. 12).

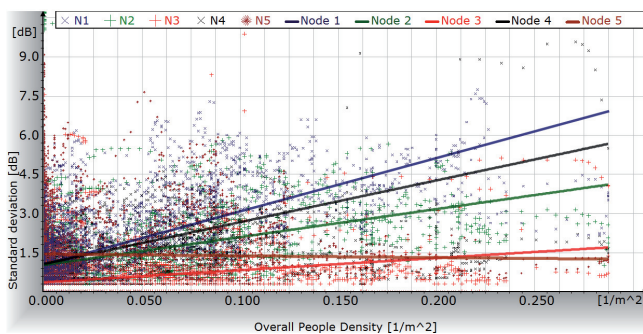


Fig. 12. Standard deviation for all nodes versus overall people density and extrapolated linear functions.

From the linear regression shown in Fig. 12 it is possible to express a short-term fading from the standard deviation, related to the overall people density:

$$L_S[\text{dB}] = 1.64 \cdot (k + \alpha \cdot \rho_{All}) \quad (10)$$

where k is the short-term fading expressed with no present people (Tab. 3) and α is the slope of the short-term fading regression. Empirical results of these coefficients derived from the measurements are shown in Tab. 4.

Node ID	k [dB]	α [dB m ²]	Conditions
1	1,02	20,4	NLOS
2	1	10,7	LOS
3	0,36	4,6	LOS
4	1,1	16	NLOS
5	1,4	-0,68	NLOS

Tab. 4. Short-term fading coefficients for different nodes.

For nodes 1 to 4, the regression of standard deviation with the overall people density is clearly expressed, whereas for the node 5 which is not located within the testbed, the regression shows almost constant short-term fading, representing no correlation with the measurements. This can be seen from the following, Fig. 11 and Fig. 12 respectively. Further on, the NLOS conditions suffers mostly from the impact of human presence, whereas in LOS condition this effect is mitigated. Exemption is node 2 at near NLOS conditions. The extent of α depends mostly on the propagation conditions (LOS or NLOS) and the probability of human presence in the area of 1st Fresnel zone. These results can be corroborated from the experiments conducted in [4], where the overall impact of human presence in LOS and NLOS conditions is given. As opposed to the approach given in [4], this paper takes into consideration people density.

Next on, the long term fading is expressed by using average values of the received signal strength. As seen from Fig. 9, the average value correlates with the people density but not as strong as standard deviation. The correlation coefficients are shown in Fig. 13.

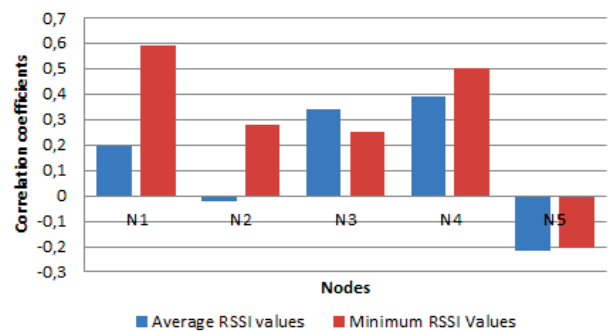


Fig. 13. Correlation coefficients for Average and Minimum RSSI values against human density.

As displayed in Fig. 13, the average RSSI values does not follow the correlation as well as standard deviation does. On the other hand, if a minimum value of each data window is plotted and the correlation between minimum values and the people density is calculated, this correlation follows the correlation of the standard deviation. This can be seen from Fig. 13.

The reason behind these results is: The fact that the long term fading is caused by people shadowing in the propagation path can be seen from the samples when a large number of people occupies the area. In this scenario the RF propagation is shadowed by human presence and this effect is seen as a drop in average RSSI values. On the

other hand, when people density is lower, statistically the probability that persons could completely shadow the RF propagation is reduced. This effect is especially expressed in NLOS conditions and areas with highest human activity. In the presented testbed the area of most activity is the propagation path of node 4, being the foyer of a student classroom. Having this in mind, the highest impact of human presence on long term fading is seen on this node.

If the same linear regression is applied to the difference between instantaneous and average values the impact of human presence is clearly seen in NLOS conditions for nodes 1 and 4. Nodes in LOS conditions do not seem to be influenced by the human presence. It can be concluded that nodes in LOS conditions do not suffer the influence of human presence, not to a degree that could compromise normal WSN operation. On the other hand, nodes in NLOS conditions suffer greatly from the impacts of long term fading. This is seen from node 4, being in worst case scenario.

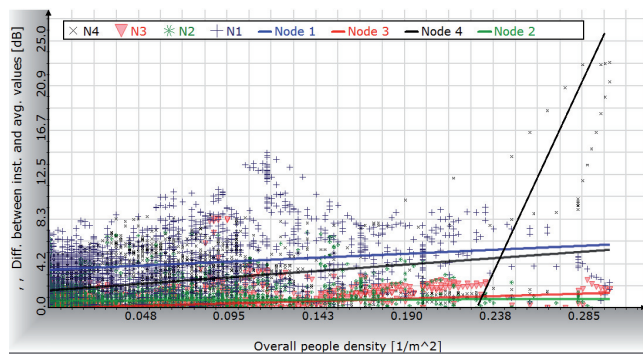


Fig. 14. RSSI delta values with linear extrapolated functions versus people density.

From Fig. 14 it can be concluded that long term fading is only dominant for node 4 being in worst case scenario. The impact of long term fading for this node is not negligible, as in some cases it exceeds 23 dB in value. This effect can cause signal outages and loss of data. Further on, it can be seen that this effect is only dominant when people density exceeds a certain limit. In the case of node 4 this limit is 0.22 m⁻² or 1.4 people per the 1st Fresnel area. If compared to results in [5], the impact of 1 person in the propagation path results in drop of RSSI by 9 dB, whereas in this case the impact is 8.8 dB, corroborating given values. If a linear extrapolation is given, setting the limit for long term fading as more than 1 person per the 1st Fresnel area, and the slope being $s = 9$ dB/person, the relation is:

$$L_L[\text{dB}] = s \cdot \lfloor \rho_n \cdot A_n \rfloor \quad (11)$$

where ρ_n is the people density for node n , A_n is the area of the 1st Fresnel zone defined according to (6), and s is the slope (9 dB/person for NLOS and 0 dB/person for LOS conditions). For LOS conditions, long-term fading in correlation with people density can be neglected, as human presence causes no severe signal drops, thus eliminating the possibility for signal outage and data loss.

From the results obtained within this study it is possible to define an empirical fading margin prediction model, dependent mostly on people density per m² and propagation conditions. According to (3) the fading margin can be defined as:

$$F[\text{dB}] = 1.64 \cdot (k + \alpha \cdot \rho_{All}) + s \cdot \lfloor \rho_n \cdot A_n \rfloor \quad (12)$$

where the coefficients k , α and s are given in Tab. 5, ρ_{All} is the overall people density and A_n is the number of people occupying the 1st Fresnel zone of a node n .

Coefficient	Line Of Sight	Non Line Of Sight
k [dB]	0.0 – 1.0	1.0 – 2.0
α [dB m ⁻²]	4.0 – 11.0	15.0 – 25.0
s [dB/person]	0	8.0 – 9.0

Tab. 5. Fading prediction coefficients.

The range of coefficients depends on real life conditions and can be ascertained upon real life WSN deployment. By proposing this method of WSN deployment it is possible to intelligently plan the WSN resulting in reduction of power consumption, reduction of RF spectrum contamination and minimizing the risk of RF impact on human health by means of restricting the transmit power of a wireless sensor network module.

6. Conclusions and Future Work

The main goal of this paper was empirical determination of the fading margins for real life WSN deployment in indoor scenarios. The reason for determining fading margin is the ability to plan WSN links using link budget analysis in the pursuit of reducing transmit and Equivalent Isotropically Radiated Power (EIRP). This leads to power consumption reduction and spectrum contamination minimization. Another important aspect analyzed in this paper was the influence of people density per m² on the RF propagation, specifically the influence on short term and long term fading. From the scope of this paper, it was concluded that the human presence in the area of RF propagation significantly influences the propagation, as human bodies present an obstacle to the RF signal. It was concluded that the nodes exhibiting LOS (line-of-sight) propagation do not suffer from the problems of human presence, namely because the dominant ray is rarely completely shadowed. On the other hand, due to no wall attenuations the signal strength for these nodes is significantly higher, statistically eliminating the ability for human presence to cause a signal outage and data loss.

Next on, the impact of human presence on short term fading was shown to be more emphasized for nodes with NLOS conditions than for nodes with LOS conditions. The correlation analysis revealed a high correlation between standard deviation and human density (number of people in the observed area). Further on, it was shown that the short term fading exhibits a linear dependence and a rising trend compared to the people density. For nodes with NLOS

conditions this trend is more emphasized than for nodes with LOS conditions. Nodes that are not affected with human presence show a constant magnitude of short term fading.

On the other hand, long term fading is a direct consequence of human presence, as human body representing a shadowing obstacle to the RF signal. Since long term fading requires complete shadowing of RF propagation path, this effect is only expressed when more than one person is located within the propagation path. From this and related work it was concluded that long term fading is mostly responsible for signal outages in NLOS conditions, whereas in LOS conditions this effect can be neglected (as it causes neither signal outages nor drop in received data). For NLOS conditions long term fading margin was mathematically modeled, being dependent on people density. Altogether, the empirical model for fade margin prediction was proposed with the given range of coefficients, enabling real life WSN deployment use.

Future work includes analyzing possible fading models for various scenarios and modeling a universal empirical fading model that could be applied to every deployment scenario. The analysis of the nature of the coefficients is also planned, examining various real life deployment parameters, such as building type. Also, in conjunction with the concept of Adaptive Transmit Power Control it is possible to implement a dynamic transmit power control algorithm based on the calculated fading margin, guaranteeing no signal outages and a high probability data reception rate.

Acknowledgement

This work was sponsored by the Ministry of Science, Education and Sports of the Republic of Croatia under projects 165-0362027-1479 and 165-0361630-1636.

References

- [1] CHOWDHURI, S., MONDAL, A. Fading analysis of MIMO based mobile ad-hoc networks. *International Journal of Distributed and Parallel Systems*, 2011, vol. 2, no. 4, p. 35-41.
- [2] LOYKA, S., KOUKI, A. B., GAGNON, F. Fade depth prediction on wireless microwave links using two-ray multipath model. In *Proceedings of 2001 Canadian Conference on Electrical and Computer Engineering (CCECE 2001)*. Toronto (Canada), May 13-16, 2001, p. 493-498.
- [3] CHEHRI, A., MOUFTAH, H., FORTIER, P. RF Link budget analysis at 915 MHz band for Wireless Sensor Networks. *International Journal of Electrical and Computer Engineering*, 2010, vol. 3, no. 3, p. 281-286.
- [4] ELYES, B. H., GUILLAUME, C. Investigating the impact of human activity on the performance of wireless networks — An experimental approach. In *Proceedings of IEEE International Symposium on a World of Wireless Mobile and Multimedia Networks (WoWMoM)*, 14-17 June 2010, p. 1-8.
- [5] SU, W., ALZAGHAL, M. Channel propagation characteristics of wireless MICAz sensor nodes. *Ad Hoc Networks*, Aug. 2009, vol. 7, no. 6, p. 1183-1193.
- [6] LLANO, G., REIG, J., RUBIO, L. Analytical approach to model the fade depth and the fade margin in UWB channels. *IEEE Transactions on Vehicular Technology*, Nov. 2010, vol. 59, no. 9, p. 4214-4221.
- [7] KARTHIGA, G. Performance analysis of shadow fading with greedy approach in wireless sensor networks. *International Journal of Electronics & Communication Technology*, 2012, vol. 3, no. 1, p. 238-241.
- [8] KLEPAL, M., MATHUR, R., MCGIBNEY A., PESCH, D. Influence of people shadowing on optimal deployment of WLAN access points. In *Proceedings of IEEE 60th Vehicular Technology Conference VTC2004*, 2004, vol. 00, no. C, p. 4516-4520.
- [9] LAKKUNDI, V., KRÄTZIG, M. Wireless sensor networks: VAN-project perspectives. *Radioengineering*, June 2009, vol. 18, no. 2, p. 215-222.
- [10] SHIN, S. Y., PARK, H. S., KWON, W. H. Mutual interference analysis of IEEE 802.15.4 and IEEE 802.11b. *Computer Networks*, Aug. 2007, vol. 51, no. 12, p. 3338-3353.
- [11] PUCCINELLI, D., HAENGGI, M. Multipath fading in wireless sensor networks: Measurements and interpretation. In *Proceedings of the 2006 International Conference on Wireless Communications and Mobile Computing, IWCMC '06*, 2006.
- [12] *XBee®/XBee-PRO® ZB RF Modules Datasheet*. [Online] Cited 2012-01-21. Available at: www.digi.com.
- [13] HYNICICA, O., KACZ, P., FIEDLER, P., BRADAC, Z., KUČERA, P., VRBA, R. The ZigBee experience. In *Proceedings of the Second International Symposium on Communications, Control and Signal Processing ISCCSP2006*. Marrakech (Morocco), March 2006.
- [14] HORVAT, G., ŠOŠTARIĆ, D., ŽAGAR, D. Response surface methodology based power consumption and RF propagation analysis and optimization on XBee WSN Module. *Telecommunication Systems*. Accepted for publishing, February 2013.
- [15] FREEMAN, R. L. *Radio System Design for Telecommunications*. John Wiley & Sons, 1997.
- [16] LOTT, M., FORKEL, I. A multi-wall-and-floor model for indoor radio propagation. In *Proceedings of Vehicular Technology Conference*. 2001 Spring. IEEE VTS. 53rd.
- [17] *Choosing an XBee Antenna*. [Online] Cited 2012-05-3. Available at: <http://www.digi.com/technology/rf-tips/2007/08>.
- [18] Antenna design specifications (2.4GHz antenna)
- [19] VELIPASALAR, S., YING-LI TIAN, HAMPAPUR, A. Automatic counting of interacting people by using a single uncalibrated camera. In *Proceedings of IEEE International Conference on Multimedia and Expo.*, 9-12 July 2006, p.1265-1268.
- [20] FEHR, D., SIVALINGAM, R., MORELLAS, V., PAPANIKOLOPOULOS, N., LOTFALLAH, O., YOUNGCHOON PARK. Counting people in groups. In *Proceedings of Advanced Video and Signal Based Surveillance*. 2-4 Sept. 2009, p.152-157.
- [21] BOR, M., WOLF, E. *Principles of Optics*. Cambridge, United Kingdom: Cambridge University Press, 1999.
- [22] DIGHAM, F. F., ALOUINI, M.-S. Outage probability of selection combining in an exponentially correlated lognormal shadowing environment. In *Proceedings of the 5th Nordic Signal Processing Symposium*. Tromso (Norway), October 2002.

- [23] KELIF, J. M, COUPECHOUX, M. Joint impact of pathloss shadowing and fast fading - An outage formula for wireless networks. In *Proceedings of CoRR*. 2010.
- [24] MINIHOLD, R. RF fading simulation, A signal analyzer and vector signal generator with digital baseband interfaces combine for testing wireless devices and airborne radio. In *Proceedings of Test & Measurement World*, July 2010.

About Authors ...

Goran HORVAT received his BSc. and MSc. degree in Electrical Engineering in 2008 and 2010, respectively, both from J.J. Strossmayer University of Osijek, Faculty of Electrical Engineering. The title of his Master's thesis was "Wireless RFID user authorization". During his study, Goran Horvat won a national scholarship for gifted and talented students and completed his study with Summa cum laude qualifications. Since 2011 Mr Horvat has been working as a research associate at the Faculty of Electrical Engineering, University of Osijek, on the project "Broadband and Internet services in rural areas". The main areas of his research include wireless (multimedia) sensor networks, embedded systems, communication protocols, vehicular electronics and multi-agent systems. He has published a number of papers on his research subjects and served as a reviewer for a number of articles. Since 2013 Mr. Horvat is an editorial assistant at International Journal of Advanced Computing Research. He is a member of IEEE.

Snježana RIMAC-DRLJE received the B.S., M.S. and Ph.D. in Electrical Engineering from the University of Zagreb, Faculty of Electrical Engineering and Computing, in 1987, 1994 and 2000, respectively. Since 1987 she has been a Faculty Member at the Faculty of Electrical Engineering, University of Osijek, where she was Vice-Dean for Science from 2001 to 2003 and Vice-Dean for Educa-

tion from 2003 to 2005. Currently, she is a Full Professor in the Department of Communications and a head of the Laboratory for HF measurements. At University of Osijek, she developed and currently teaches communications systems, multimedia techniques and mobile communications. Since 2005 she is a collaborating member of the Croatian Academy of Engineering and a member of the Croatian Standards Institute Technical Committee. Also, she is a member of several associations such as IEEE, ELMAR and KOREMA. Dr. Rimac-Drlje research interests include image and video compression, wavelet transform, signal/image/video processing and digital communication systems.

Drago ŽAGAR received his BSc, MSc and PhD degree from University of Zagreb, Faculty of Electrical Engineering and Computing, in 1990, 1995, 2002, respectively. In 1995/1996 he was granted a degree of Euro Laser Engineer from the Euro Laser Academy, Technical University of Vienna. Since 1990 he has been affiliated with the Department of Communications, Faculty of Electrical Engineering, University of Osijek, where he has reached a rank of full professor. He was Head of the Communications Laboratory (2001-2005), and since 2006 he is Head of the Communications Department at the Faculty of Electrical Engineering, University of Osijek. From 2003 to 2005 he was Vice-Dean for Education, and currently he is Vice-Rector for Education and Students at the University of Osijek. In 2013 Dr. Žagar was elected for the function of the Dean of the Faculty of Electrical Engineering Osijek to a four-year term. He has been engaged in many research and professional projects, as well as several TEMPUS projects. His main research interests include Quality of Service in IP networks, formal methods for protocol verification, computer networks and network security. Dr. Žagar is a member of IEEE and ACM (Association for Computing Machinery).